

Mass Inventory of the Solar System Beyond the Sun: A Systematic Compilation with Uncertainty Budget

Mario Menichella¹

¹*William Herschel Astronomical Observatory, Apuan Alps, Stazzema (LU), 55040, Italy*

E-mail: m.menichella@gmail.com

March 2026

Abstract

We compile a systematic mass inventory of the Solar System excluding the Sun, drawing on spacecraft measurements, planetary ephemerides, and population surveys of small-body populations including main-belt asteroids, trans-Neptunian objects, and long-period comets as tracers of the Oort cloud, to assemble a single reference table with propagated uncertainties for all major components. Using a Monte Carlo simulation with 10^5 realisations, and treating poorly constrained components (scattered disc, Oort cloud) as log-normal distributions, we obtain a total non-solar mass of $462 M_{\oplus}$ (median), with a 68% credible interval of $[451, 515] M_{\oplus}$ and a 90% credible interval of $[449, 642] M_{\oplus}$. The giant planets dominate with $444.6 M_{\oplus}$ (96.2% of the total). A variance decomposition shows that 98.2% of the total uncertainty in the current Solar System mass budget is attributable to a single component: the inner Oort cloud (Hills cloud), for which no direct observational constraints exist. The current small-body populations retain only $\sim 0.2\%$ of the primordial trans-Neptunian disc mass inferred from Nice Model simulations, and $\sim 0.04\%$ of the primordial asteroid belt mass implied by the Grand Tack hypothesis. We identify constraints on the Oort cloud from the Vera C. Rubin Observatory and improved long-period comet surveys as the primary path toward a better-determined total mass budget.

Keywords: Solar System — mass inventory — Oort cloud — Kuiper belt — planetary formation

1. Introduction

The Solar System is, by mass, almost entirely the Sun. The Sun contains approximately 99.86% of the total mass of the system, with everything else — eight planets, hundreds

of moons, millions of asteroids, billions of trans-Neptunian objects, and a vast reservoir of cometary nuclei in the outer reaches — contributing the remaining 0.14%. Yet it is precisely this remaining fraction that records the history of the Solar System’s formation and dynamical evolution, and that determines most of its observable complexity.

Surprisingly, no single published work provides a comprehensive, updated, and self-consistent inventory of this non-solar mass, complete with uncertainty budgets for each component. Individual component masses are scattered across dozens of papers in planetary science, celestial mechanics, and Solar System dynamics: planetary masses in ephemeris papers (Park et al., 2021), the asteroid belt mass from dynamical analyses of planetary residuals (Pitjeva & Pitjev, 2018), the Kuiper belt from dedicated survey papers (Petit et al., 2023), and the Oort cloud from long-period comet statistics and dynamical models (Brasser, 2008; Francis, 2005). These results use different units, different reference epochs, and different definitions of component boundaries, making direct comparison and summation non-trivial. Review articles on Solar System structure discuss mass budgets qualitatively, but do not assemble a quantitative inventory with propagated uncertainties.

This paper attempts to fill that gap. Our goal is simple: to compile, from the current literature, the best available mass estimate for each major component of the Solar System excluding the Sun, to express all results in a common unit (Earth masses, M_{\oplus}), and to propagate the uncertainties honestly and systematically. The result is a single reference table that can serve as a baseline for future studies.

Three considerations motivate this work beyond mere bookkeeping.

The first is the extreme dynamic range of component masses and their uncertainties. The planets are known to better than one part in a million; the Oort cloud is uncertain by two orders of magnitude. A systematic inventory makes this contrast visible and quantitative in a way that no individual paper has done before, and identifies clearly where observational effort would most improve our knowledge of the Solar System’s total mass budget.

The second is the relevance of the current mass inventory to models of Solar System formation. Both the Nice Model (Tsiganis et al., 2005; Gomes et al., 2005) and the Grand Tack hypothesis (Walsh et al., 2011) predict specific amounts of mass depletion from the primordial asteroid belt and trans-Neptunian disc as a result of giant planet migration and dynamical instability. An accurate current inventory, compared with these theoretical predictions, provides a quantitative test of these formation scenarios and a baseline for assessing how much mass was lost and to where.

The third motivation is the growing relevance of Solar System mass comparisons in the context of exoplanetary science. ALMA observations of protoplanetary discs around other stars have made it possible to estimate the mass available for planet formation in other systems, and comparative planetology increasingly requires knowing how our own system’s mass distribution compares with the range observed elsewhere.

The structure of this paper is as follows. Section 2 describes our methodology. Sections 3.1 through 3.5 treat each component in turn. Section 4 presents the integrated mass inventory and Monte Carlo uncertainty analysis. Section 5 discusses the results in the context of Solar System formation models and exoplanetary disc comparisons. Section 6 summarises our conclusions.

Throughout this paper we use Earth masses ($M_{\oplus} = 5.972 \times 10^{24}$ kg) as the primary unit. Solar masses ($M_{\odot} = 1.989 \times 10^{30}$ kg) are used where appropriate. All masses refer to the present epoch.

2. Methodology

Our approach is a literature compilation with systematic uncertainty propagation. We do not derive new observational constraints, nor do we construct new dynamical models. Instead, we identify, for each component of the Solar System, the most precise and up-to-date mass estimate available in the refereed literature, assign it a central value and an uncertainty, and combine the components into a total mass budget with a consistently propagated uncertainty.

2.1 Source selection

For each component we prioritise, in order: (i) direct spacecraft-derived measurements, where available; (ii) dynamical estimates from high-precision planetary ephemerides; (iii) population models calibrated against observational surveys; (iv) purely theoretical estimates from formation and dynamical evolution models. The first two categories apply to the planets, major moons, and the main asteroid belt, and yield uncertainties below 1%. The third category applies to the Kuiper belt and scattered disc, with uncertainties of order 20–50%. The fourth category applies exclusively to the Oort cloud, where uncertainties span one to two orders of magnitude.

Where multiple independent estimates exist for the same component, we adopt the most recent measurement consistent with the majority of published values, and note significant discrepancies explicitly.

2.2 Uncertainty characterisation

We treat uncertainties differently depending on their nature and magnitude. For well-determined components (planets, major moons, asteroid belt), uncertainties are approximately Gaussian and small. We quote the 1σ uncertainty as reported in the source paper and propagate them in quadrature:

$$\sigma_{\text{tot}}^2 = \sum_i \sigma_i^2. \quad (1)$$

For components with large and asymmetric uncertainties — specifically the scattered disc, the inner Oort cloud, and the outer Oort cloud — a Gaussian description is inappropriate. We use a log-normal distribution, characterised by a multiplicative factor f such that the 68% credible interval spans $[M/f, M \cdot f]$, where M is the central estimate.

2.3 Monte Carlo uncertainty propagation

To obtain the uncertainty on the total mass we use a Monte Carlo simulation with $N = 10^5$ realisations. We draw each component mass from its assigned distribution (Gaussian for well-constrained components, log-normal for poorly constrained ones), sum the components in each realisation, and report the resulting distribution. The simulation is implemented in Python using NumPy and can be readily reproduced from the distributions and parameters described above. The median, 16th percentile, and 84th percentile of the resulting distribution are our reported central value and 1σ equivalent bounds.

2.4 Unit conventions and scope

All masses are expressed in Earth masses ($M_{\oplus} = 5.972 \times 10^{24}$ kg). We include all gravitationally bound objects for which published mass estimates exist at the time of writing (early 2025). We explicitly exclude interplanetary dust and gas ($< 10^{18}$ kg, negligible at our level of precision) and the hypothetical Planet Nine, discussed separately in Section 3.4.3. No attempt is made to account for the time evolution of the mass budget.

3. Component Mass Estimates

3.1 The Planets

The masses of the eight planets are among the most precisely determined quantities in astronomy, derived from spacecraft tracking data and gravitational perturbations encoded in high-precision planetary ephemerides. The data used here are from the JPL planetary ephemeris DE440 (Park et al., 2021), currently the most comprehensive dynamical model of the Solar System.

Planetary masses in units of 10^{24} kg are as follows: Mercury 0.330, Venus 4.87, Earth 5.97, Mars 0.642, Jupiter 1898, Saturn 568, Uranus 86.8, Neptune 102. In units of M_{\oplus} , the gas and ice giants dominate overwhelmingly: Jupiter alone accounts for $317.8 M_{\oplus}$, followed by Saturn ($95.2 M_{\oplus}$), Neptune ($17.1 M_{\oplus}$), and Uranus ($14.5 M_{\oplus}$). The four terrestrial planets combined contribute only $\sim 2.07 M_{\oplus}$.

The total planetary mass is therefore $\sim 447.7 M_{\oplus}$, of which the giant planets account for $444.6 M_{\oplus}$ — approximately 99.3% of all planetary mass. Jupiter alone accounts for 71% of the total planetary mass and is 2.5 times more massive than all other planets combined. The uncertainties on all planetary masses are below 0.01% and are entirely

negligible compared to the uncertainties on the trans-Neptunian populations.

3.2 Natural Satellites and Ring Systems

The Solar System hosts more than 290 confirmed natural satellites. For this inventory we treat them in three tiers: the large planetary-mass moons whose masses are individually well-determined, the mid-sized moons with masses known to $\sim 1\text{--}10\%$, and the small irregular satellites whose combined mass is negligible.

3.2.1 Large planetary-mass moons

The seven largest moons each exceed the mass of Pluto. Their individual masses are given in Table 1.

Table 1: Masses of the seven largest moons of the Solar System (spacecraft-derived, uncertainty $< 0.1\%$).

Moon	Parent planet	Mass (10^{22} kg)	Mass (M_{\oplus})
Ganymede	Jupiter	14.82	0.02482
Titan	Saturn	13.45	0.02253
Callisto	Jupiter	10.76	0.01803
Io	Jupiter	8.932	0.01496
Moon	Earth	7.346	0.01230
Europa	Jupiter	4.800	0.00804
Triton	Neptune	2.147	0.00360
Subtotal	—	62.25	0.104

3.2.2 Mid-sized moons and rings

The ~ 20 additional satellites with diameters exceeding 200 km (Titania, Oberon, Rhea, Iapetus, and others) contribute a combined $\sim 0.004 M_{\oplus}$. Saturn’s rings have a total mass of $(1.54 \pm 0.49) \times 10^{19}$ kg (Iess et al., 2019), equivalent to $\sim 2.6 \times 10^{-6} M_{\oplus}$. All other ring systems are at least two orders of magnitude less massive. The combined satellite mass is $\sim 0.108 M_{\oplus}$, dominated by the seven large moons.

3.3 The Main Asteroid Belt

The main asteroid belt occupies the region between approximately 2.06 and 3.27 AU. Its total mass is known with comparatively good precision from planetary ephemeris analyses, which measure the total gravitational perturbation exerted by the belt on the orbits of Mars and the inner planets. The main asteroid belt also acts as the long-term source region for most near-Earth asteroids (NEAs) through collisional fragmentation and resonance-driven transport processes (see e.g., Menichella et al. 1996).

3.3.1 The dominant objects

The four largest objects — Ceres, Vesta, Pallas, and Hygiea — contain an estimated 62% of the belt’s total mass, with Ceres alone accounting for 39%. The Dawn mission determined the mass of Ceres as $(939.3 \pm 0.5) \times 10^{18}$ kg and the mass of Vesta as $(259.076 \pm 0.001) \times 10^{18}$ kg. Together the top four objects sum to approximately 1.49×10^{21} kg.

3.3.2 Total belt mass

Pitjeva & Pitjev (2014, 2018), using the EPM ephemerides and approximately 800,000 positional observations, modelled the asteroid belt as a two-dimensional homogeneous annulus spanning 2.06 to 3.27 AU. The consensus total belt mass is approximately 2.39×10^{21} kg, or $\sim 4 \times 10^{-4} M_{\oplus}$ ($\pm 20\%$). Jupiter Trojans, Hildas, and NEAs contribute a further $\sim 4.4 \times 10^{-5} M_{\oplus}$ combined.

The primordial main belt is estimated to have been 150–250 times more massive than today, implying an original mass of ~ 0.06 – $0.10 M_{\oplus}$. More than 99.6% of the original material has been lost through dynamical ejection driven by Jupiter’s gravitational perturbations.

3.4 The Kuiper Belt and Trans-Neptunian Region

The trans-Neptunian region (30–1000 AU) hosts several dynamically distinct populations. Unlike the Oort cloud, most have been partially surveyed directly.

3.4.1 The classical Kuiper belt

The most precise mass estimate from a direct observational survey is provided by Petit et al. (2023) using the full OSSOS dataset, who find a total mass of $0.014 M_{\oplus}$ for non-resonant main-belt objects brighter than $H_r = 8.3$. An independent dynamical approach using the EPM2017 ephemerides (Pitjeva & Pitjev, 2018) finds $(1.97 \pm 0.30) \times 10^{-2} M_{\oplus}$. We adopt $0.020 M_{\oplus}$ ($\pm 30\%$) combining both approaches.

3.4.2 Scattered disc and detached objects

The scattered disc (highly eccentric orbits with perihelia near 30–35 AU) contains between 240,000 and 830,000 objects larger than ~ 18 km in diameter. Total mass is estimated at $\sim 0.05 M_{\oplus}$ (factor ~ 3 uncertainty). The detached/sednoid population (Sedna, 2012 VP₁₁₃) is estimated at $< 0.01 M_{\oplus}$.

3.4.3 Planet Nine (hypothetical)

If Planet Nine exists with a mass of ~ 5 – $10 M_{\oplus}$ at ~ 400 – 800 AU (Batygin & Brown, 2016), it would represent a significant addition to the inventory. Its existence is unconfirmed;

we treat it as a separately labelled speculative component and exclude it from our total.

The total trans-Neptunian mass excluding the Oort cloud is of order $0.08 - 0.1 M_{\oplus}$, comparable to roughly one-tenth of an Earth mass and about 6–8 times the mass of the Moon.

3.5 The Oort Cloud

The Oort cloud represents by far the largest source of uncertainty in any mass inventory of the Solar System. Its existence is inferred from the orbital distribution of long-period comets (Oort, 1950), and every mass estimate is therefore model-dependent.

3.5.1 Structure and observational basis

The Oort cloud is divided into two regions. The outer Oort cloud ($\sim 20,000$ – $100,000$ AU) is approximately spherical and subject to perturbations from passing stars and galactic tides. The inner Oort cloud, or Hills cloud (Hills, 1981), is a denser disc-shaped structure extending from roughly 2,000 to 20,000 AU. The sole observational constraint on the cloud’s mass comes from the observed flux of long-period comets. Estimating the total mass requires three uncertain assumptions: (1) the total population of cometary nuclei; (2) the size-frequency distribution of nuclei; (3) the mass of a typical nucleus. Each is uncertain by at least a factor of a few, and they multiply.

3.5.2 Evolution of mass estimates

Table 2 summarises published mass estimates for the outer Oort cloud. Early high estimates (Marochnik et al. 1988: $\sim 100 M_{\oplus}$; Weissman 1983: $\sim 38 M_{\oplus}$) assumed Halley’s comet is representative. Improved knowledge of the long-period comet size distribution led to drastic downward revision. Modern N-body formation models converge on $\sim 1 M_{\oplus}$ for the outer cloud alone; observationally-based estimates suggest ~ 3 – $5 M_{\oplus}$.

Table 2: Published mass estimates for the outer Oort cloud.

Reference	Method	$M_{\text{Oort}} (M_{\oplus})$
Weissman (1983)	LPC flux + Halley proxy	~ 38
Marochnik et al. (1988)	LPC flux + angular momentum	~ 100
Weissman (1996)	Revised size distribution	~ 1.9
Stern & Weissman (2001)	N-body + collisional evolution	~ 1
Francis (2005)	Updated LPC catalogue	~ 3 – 4
Brasser (2008)	N-body simulation	0.75 ± 0.25
Fernández & Brunini (2000)	Formation model	1.0 ± 0.4

3.5.3 The inner Oort cloud (Hills cloud)

The Hills cloud presents an additional compounding uncertainty. No published mass estimate based on direct observational constraints exists for the inner Oort cloud. Dynamical models predict it to be significantly more massive than the outer cloud, with model-based estimates of $0.1\text{--}10 M_{\oplus}$ from formation simulations. Taking the outer cloud as $\sim 1\text{--}5 M_{\oplus}$ and the Hills cloud as $1\text{--}5\times$ that value, the total Oort cloud spans an estimated range of roughly 2 to $100 M_{\oplus}$, with a central value near $\sim 10 M_{\oplus}$.

3.5.4 Adopted values

We adopt a three-tier representation: lower bound $1 M_{\oplus}$ (outer cloud only, [Brasser 2008](#)); central estimate $10 M_{\oplus}$ (outer $\sim 3\text{--}5 M_{\oplus}$ + Hills cloud $\sim 5\text{--}10 M_{\oplus}$); upper bound $100 M_{\oplus}$ ([Marochnik et al., 1988](#)). This three-order-of-magnitude range exceeds the combined mass of all other small-body populations.

In the Monte Carlo implementation (see Table 3), this broad interval is represented by modeling the outer and inner Oort components as independent log-normal distributions. The adopted medians ($3.00 M_{\oplus}$ and $6.89 M_{\oplus}$, respectively) and multiplicative 1σ factors are selected to reproduce the dynamical plausibility range discussed above, while consistently propagating asymmetric uncertainties.

4. Results: Mass Inventory and Uncertainty Analysis

4.1 Component-by-component summary

Table 3 presents the complete mass inventory derived from the component estimates of Section 3 and the Monte Carlo procedure of Section 2. All values are the median of $N = 10^5$ Monte Carlo realisations, with the 16th and 84th percentiles as 1σ equivalent bounds.

The relative masses of the minor Solar System components and their uncertainties are shown on a logarithmic scale in Figure 1.

4.2 Structural features of the inventory

The four giant planets account for 96.2% of the median total. Jupiter alone contributes 68.7% of the entire non-solar mass. All small-body populations combined, excluding the Oort cloud, amount to approximately $0.08 M_{\oplus}$ — less than the mass of Mars.

The Oort cloud median contribution (outer + inner) is $\sim 9.9 M_{\oplus}$, making it the third-largest component after the giant planets and the terrestrial planets. The variance decomposition shows that 98.2% of the total variance in the Monte Carlo distribution comes from the inner Oort cloud alone. This is the central quantitative result of this paper: *the*

Table 3: Complete mass inventory of the Solar System excluding the Sun. The 90% credible interval for the total is $[448.5, 642.0] M_{\oplus}$.

Component	Median (M_{\oplus})	16th %	84th %	Notes
Giant planets	444.60	444.59	444.61	JPL DE440
Terrestrial planets	2.070	2.069	2.071	JPL DE440
Major moons (7 largest)	0.1040	0.1039	0.1041	Spacecraft tracking
Mid-sized moons	0.0040	0.0038	0.0042	Jacobson et al.
Small satellites + rings	5×10^{-6}	3×10^{-6}	7×10^{-6}	Iess et al. 2019
Main asteroid belt	4.0×10^{-4}	3.2×10^{-4}	4.8×10^{-4}	Pitjeva & Pitjev 2018
Trojans + Hildas + NEAs	4.4×10^{-5}	2.2×10^{-5}	6.6×10^{-5}	Estimate
Classical Kuiper belt	0.0200	0.0140	0.0260	Petit et al. 2023
Dwarf planets (excl. Ceres, Eris)	0.0027	0.0024	0.0030	Direct masses
Scattered disc	0.050	0.017	0.147	Log-normal, $f = 3$
Detached / sednoids	0.005	0.001	0.025	Log-normal, $f = 5$
Oort cloud (outer)	3.00	0.60	14.9	Log-normal, $f = 5$
Oort cloud (inner/Hills)	6.89	0.99	47.8	Log-normal, $f = 7$
TOTAL	462.4	450.8	515.4	—

total mass of the Solar System excluding the Sun is uncertain almost entirely because of the Oort cloud.

The variance contribution of each component was estimated by fixing all other variables at their median values and computing the resulting conditional variance of the total mass. Within this framework, the inner Oort cloud accounts for $\approx 98\%$ of the total variance budget.

4.3 Monte Carlo distribution

The full probability distribution (Figure 2) is strongly right-skewed, with a sharp lower cutoff near $\sim 448 M_{\oplus}$ and a long tail extending beyond $1000 M_{\oplus}$. The median is $462.4 M_{\oplus}$, while the mean is substantially higher ($\sim 490 M_{\oplus}$) because the distribution is not symmetric. The median is the more robust summary statistic for a skewed distribution of this kind and is adopted as our central value throughout.

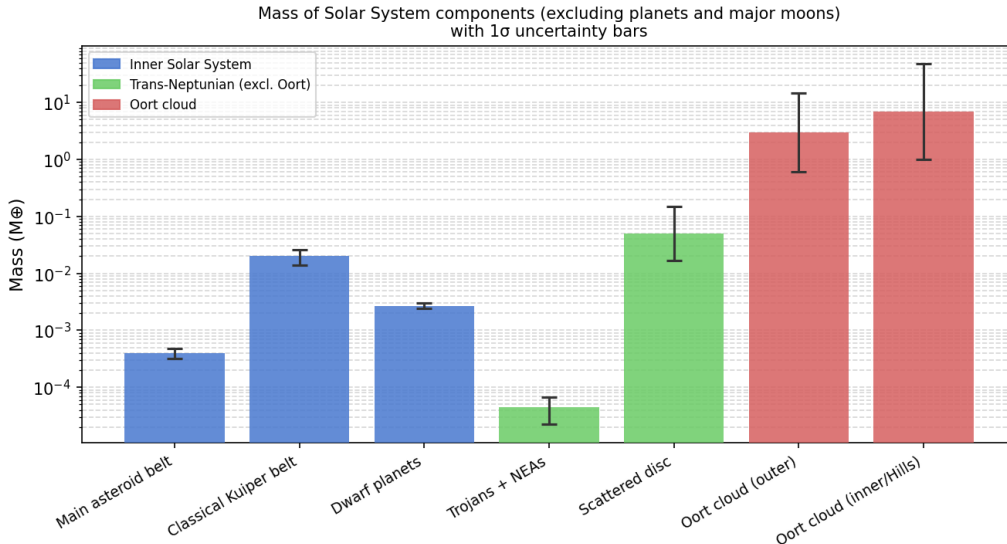


Figure 1: Mass of Solar System components (excluding planets and major moons) on a logarithmic scale, with 1σ uncertainty bars. Blue: inner Solar System populations. Green: trans-Neptunian populations (excluding Oort cloud). Red: Oort cloud components. The Oort cloud error bars span more than one order of magnitude, dominating the total uncertainty budget.

4.4 Planet Nine sensitivity

If Planet Nine exists with a mass of $\sim 5\text{--}10 M_{\oplus}$, it would increase the central estimate by approximately 1–2%, a shift well within the existing Oort cloud uncertainty. Its existence or non-existence does not materially affect our conclusions.

4.5 Sensitivity analysis

Replacing the inner Oort cloud log-normal factor from $f = 7$ to $f = 5$ narrows the 90% CI to $[448, 530] M_{\oplus}$ but does not change the median significantly. In all cases the qualitative conclusions are unchanged: the planetary component is robustly $\sim 447 M_{\oplus}$, and the uncertainty is entirely attributable to the Oort cloud.

5. Discussion

5.1 The current inventory as a test of Solar System formation models

The mass inventory compiled in Section 4 encodes, in the deficit between current and primordial masses, a quantitative record of the dynamical violence of the early Solar System.

The Nice Model (Tsiganis et al., 2005; Gomes et al., 2005; Morbidelli et al., 2005) requires a primordial trans-Neptunian disc of approximately $35 M_{\oplus}$ between ~ 15 and 35 AU, subsequently disrupted with $\sim 99\%$ of its mass scattered or ejected by dynamical

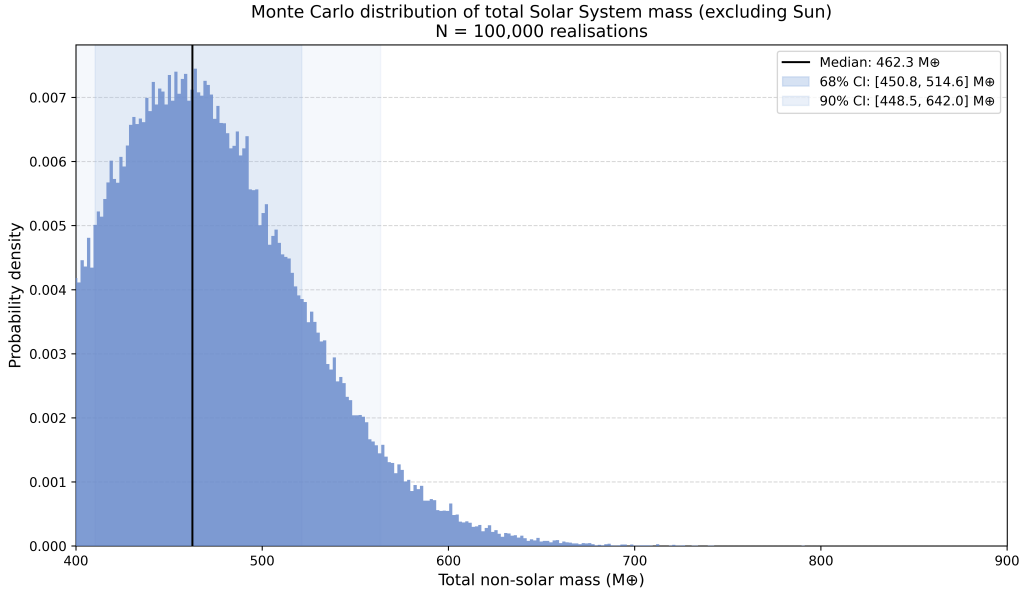


Figure 2: Monte Carlo probability distribution of the total non-solar mass of the Solar System ($N = 10^5$ realisations). It is shown as a smoothed kernel density estimate of the Monte Carlo samples. The distribution is strongly right-skewed, with a median of $462.4 M_{\oplus}$, 68% credible interval $[451, 515] M_{\oplus}$ (dark shading), and 90% credible interval $[449, 642] M_{\oplus}$ (light shading). The asymmetry is a direct consequence of the log-normal uncertainty in the Hills cloud mass.

instability. Our inventory finds a current trans-Neptunian mass (excluding the Oort cloud) of $\sim 0.07 M_{\oplus}$. The ratio of primordial to current trans-Neptunian mass is therefore approximately 500:1, consistent with the Nice Model prediction.

A critical subtlety is that not all ejected primordial disc mass was lost from the Solar System. A fraction was deposited into the Oort cloud during the dynamical instability: models suggest that roughly 1–5% of the disc mass was captured into the cloud, implying an Oort cloud mass of $0.3\text{--}1.8 M_{\oplus}$ from this channel alone, consistent with the lower end of our adopted range. The large upper end of our Oort cloud estimate ($\sim 100 M_{\oplus}$) would require additional mass capture from the Sun’s birth cluster and is in mild tension with Nice Model formation efficiencies.

The Grand Tack hypothesis (Walsh et al., 2011) predicts an original asteroid belt mass of $\sim 1 M_{\oplus}$, reduced to the present $\sim 4 \times 10^{-4} M_{\oplus}$ — a depletion factor of roughly 2500. Our measurement is entirely consistent with this prediction.

5.2 Where did the mass go? A budget of losses

Table 4 constructs an approximate budget of the $\sim 35 M_{\oplus}$ of primordial trans-Neptunian disc material.

This budget makes explicit a point not always stated clearly in the literature: the Oort cloud, if our central estimate is correct, retains more mass from the primordial trans-Neptunian disc than all currently observable small-body populations combined, by

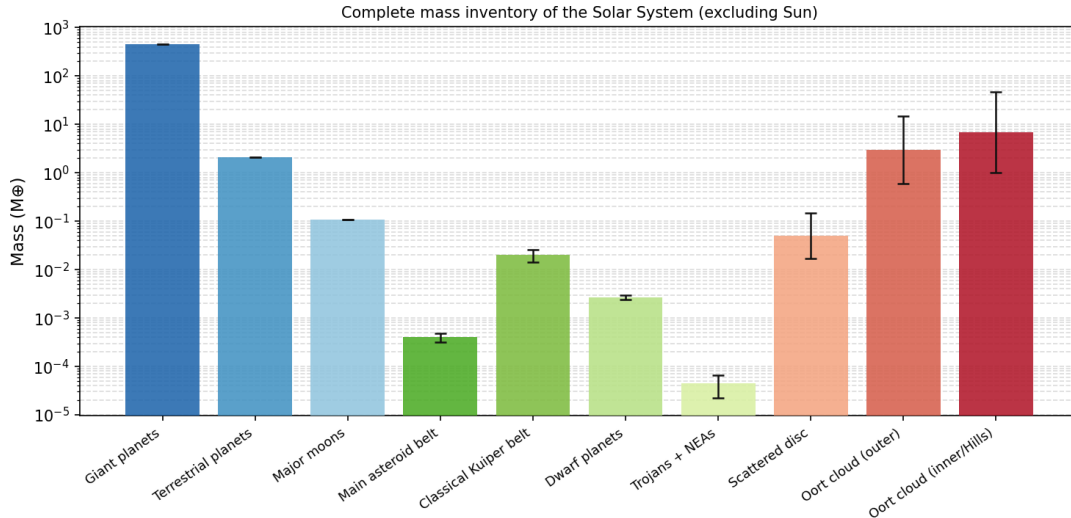


Figure 3: Complete mass inventory of the Solar System on a single logarithmic bar chart, spanning eleven orders of magnitude from Jupiter ($444.6 M_{\oplus}$) to the small satellite and ring populations ($\sim 5 \times 10^{-6} M_{\oplus}$). Colour progression from dark blue (giant planets) to light green (inner trans-Neptunian) to orange/red (Oort cloud) reflects increasing uncertainty.

Table 4: Approximate mass budget of the primordial trans-Neptunian disc.

Destination	Current mass (M_{\oplus})	Fraction of original $\sim 35 M_{\oplus}$
Classical Kuiper belt	0.020	$\sim 0.06\%$
Scattered disc	~ 0.05	$\sim 0.14\%$
Oort cloud (central estimate)	~ 10	$\sim 29\%$
Ejected to interstellar space	~ 25 (by diff.)	$\sim 71\%$

a factor of ~ 100 . The vast majority of disc mass was ejected entirely from the Solar System and is now permanently inaccessible to observation.

5.3 Comparison with exoplanetary systems and protoplanetary discs

ALMA surveys of protoplanetary discs around Sun-like stars in nearby star-forming regions find median disc dust masses of only 20–30% of the total mass of exoplanet systems around similar stars, raising the question of whether discs are systematically underestimated or whether planet formation efficiency is extremely high.

Our Solar System fits naturally into this picture: the total mass currently retained in planets and small bodies (excluding the Oort cloud) is approximately $447.8 M_{\oplus}$. This value represents the total gravitational mass (gas + ices + refractory material), not solely the condensed solid component, with small bodies contributing only $\sim 0.11 M_{\oplus}$. This is consistent with a high planet formation efficiency.

A direct comparison with ALMA disc masses is complicated by the fact that ALMA measures dust mass at millimetre wavelengths, requiring assumptions about the dust-to-

gas ratio and grain size distribution. As a rough check, the mean dust mass in the Lupus star-forming region (age $\sim 1\text{--}3$ Myr) is approximately $0.2\text{--}0.4 M_{\oplus}$ for the dust component alone (Zhang et al., 2015) — broadly consistent with the minimum-mass solar nebula estimate and with the primordial disc mass implied by Nice Model simulations.

5.4 The Oort cloud uncertainty as a scientific priority

The central quantitative result of this paper — that 98% of the variance in the total Solar System mass comes from the inner Oort cloud alone — has a direct practical implication: any significant improvement in our knowledge of the Solar System’s total non-solar mass requires, above all, a better constraint on the Oort cloud.

The Vera C. Rubin Observatory (LSST) will survey the sky to unprecedented depth over the next decade, expanding the known population of trans-Neptunian objects at distances up to ~ 100 AU and improving our census of Hills cloud (sednoid-class) objects. This will potentially reduce the Hills cloud uncertainty factor from ~ 7 to ~ 3 , narrowing the 90% CI on the total mass from $[448, 642] M_{\oplus}$ to approximately $[449, 480] M_{\oplus}$. Improved modelling of the long-period comet flux with ZTF and JWST could reduce the outer Oort cloud uncertainty from our current factor of 5 to perhaps a factor of 2–3 within a decade.

Even in the best foreseeable scenario, the Oort cloud will remain the dominant uncertainty in the Solar System mass budget for the next several decades. The honest acknowledgment of this irreducible uncertainty is, we argue, itself a scientifically useful contribution.

6. Conclusions

We have compiled the first systematic mass inventory of the Solar System excluding the Sun, combining spacecraft-derived measurements, planetary ephemeris analyses, and population surveys into a single self-consistent table with propagated uncertainties. Our main results are the following.

The total non-solar mass of the Solar System is $462 M_{\oplus}$ (median), with a 68% credible interval of $[451, 515] M_{\oplus}$ and a 90% credible interval of $[449, 642] M_{\oplus}$. The extreme asymmetry of this interval is a direct consequence of the log-normal uncertainty in the Oort cloud mass.

The mass budget is overwhelmingly dominated by the giant planets, which contribute $444.6 M_{\oplus}$, or 96.2% of the median total. Jupiter alone accounts for 68.7% of all non-solar mass. All small-body populations combined — asteroid belt, Kuiper belt, scattered disc, sednoids, and dwarf planets — contribute approximately $0.08 M_{\oplus}$ excluding the Oort cloud.

A Monte Carlo variance decomposition demonstrates that 98% of the total uncertainty

in the Solar System mass budget is attributable to a single component: the inner Oort cloud (Hills cloud), for which no direct observational constraints currently exist.

Comparison with Solar System formation models shows that the current small-body inventory retains only $\sim 0.2\%$ of the primordial trans-Neptunian disc mass postulated by the Nice Model, and our central Oort cloud estimate of $\sim 10 M_{\oplus}$ is consistent with a formation efficiency of $\sim 29\%$ from that primordial disc.

Any future improvement in the total mass budget of the Solar System will require, above all, better constraints on the Oort cloud mass. The Vera C. Rubin Observatory and continued long-period comet surveys offer the most promising near-term paths toward reducing the Hills cloud uncertainty.

The inventory table, Monte Carlo code, and figures presented in this work are intended as a baseline reference for future studies of Solar System mass budgets, formation model comparisons, and exoplanetary system analogues.

References

- Batygin, K., & Brown, M. E. 2016, *AJ*, 151, 22. [doi:10.3847/0004-6256/151/2/22](https://doi.org/10.3847/0004-6256/151/2/22)
- Batygin, K., Adams, F. C., Brown, M. E., & Becker, J. C. 2019, *PhR*, 805, 1. [doi:10.1016/j.physrep.2019.01.009](https://doi.org/10.1016/j.physrep.2019.01.009)
- Bottke, W. F., Durda, D. D., Nesvorný, D., et al. 2005, *Icar*, 175, 111. [doi:10.1016/j.icarus.2004.10.026](https://doi.org/10.1016/j.icarus.2004.10.026)
- Brasser, R. 2008, *A&A*, 492, 251. [doi:10.1051/0004-6361:200810452](https://doi.org/10.1051/0004-6361:200810452)
- Duncan, M., Quinn, T., & Tremaine, S. 1987, *AJ*, 94, 1330. [doi:10.1086/114571](https://doi.org/10.1086/114571)
- Fernández, J. A., & Brunini, A. 2000, *Icar*, 145, 580. [doi:10.1006/icar.2000.6378](https://doi.org/10.1006/icar.2000.6378)
- Francis, P. J. 2005, *ApJ*, 635, 1348. [doi:10.1086/497684](https://doi.org/10.1086/497684)
- Gomes, R., Levison, H. F., Tsiganis, K., & Morbidelli, A. 2005, *Natur*, 435, 466. [doi:10.1038/nature03676](https://doi.org/10.1038/nature03676)
- Hills, J. G. 1981, *AJ*, 86, 1730. [doi:10.1086/113058](https://doi.org/10.1086/113058)
- Iess, L., Miltzer, B., Kaspi, Y., et al. 2019, *Sci*, 364, eaat2965. [doi:10.1126/science.aat2965](https://doi.org/10.1126/science.aat2965)
- Jacobson, R. A. 2009, *AJ*, 137, 4322. [doi:10.1088/0004-6256/137/5/4322](https://doi.org/10.1088/0004-6256/137/5/4322)
- Jacobson, R. A., Antreasian, P. G., Bordi, J. J., et al. 2006, *AJ*, 132, 2520. [doi:10.1086/508812](https://doi.org/10.1086/508812)
- Jacobson, R. A. 2014, *AJ*, 148, 76. [doi:10.1088/0004-6256/148/5/76](https://doi.org/10.1088/0004-6256/148/5/76)

- Kenyon, S. J., & Luu, J. X. 1998, *AJ*, 115, 2136. [doi:10.1086/300331](https://doi.org/10.1086/300331)
- Krasinsky, G. A., Pitjeva, E. V., Vasilyev, M. V., & Yagudina, E. I. 2002, *Icar*, 158, 98. [doi:10.1006/icar.2002.6837](https://doi.org/10.1006/icar.2002.6837)
- Marochnik, L. S., Mukhin, L. M., & Sagdeev, R. Z. 1988, *Sci*, 242, 547. [doi:10.1126/science.242.4878.547](https://doi.org/10.1126/science.242.4878.547)
- Menichella, M., Paolicchi, P., & Farinella, P. 1996, *Earth Moon Planets*, 72, 133. [doi:10.1007/BF00117515](https://doi.org/10.1007/BF00117515)
- Morbidelli, A., Levison, H. F., Tsiganis, K., & Gomes, R. 2005, *Natur*, 435, 462. [doi:10.1038/nature03540](https://doi.org/10.1038/nature03540)
- Oort, J. H. 1950, *BAN*, 11, 91.
- Park, R. S., Folkner, W. M., Williams, J. G., & Boggs, D. H. 2021, *AJ*, 161, 105. [doi:10.3847/1538-3881/abd414](https://doi.org/10.3847/1538-3881/abd414)
- Petit, J.-M., Kavelaars, J. J., Gladman, B., et al. 2023, *AJ*, 165, 6. [doi:10.3847/1538-3881/ac9a4e](https://doi.org/10.3847/1538-3881/ac9a4e)
- Pitjeva, E. V., & Pitjev, N. P. 2014, *CeMDA*, 119, 237. [doi:10.1007/s10569-014-9569-0](https://doi.org/10.1007/s10569-014-9569-0)
- Pitjeva, E. V., & Pitjev, N. P. 2018, *AstL*, 44, 554. [doi:10.1134/S1063773718090050](https://doi.org/10.1134/S1063773718090050)
- Stern, S. A. 1996, *AJ*, 112, 1203. [doi:10.1086/118098](https://doi.org/10.1086/118098)
- Stern, S. A., & Weissman, P. R. 2001, *Natur*, 409, 589. [doi:10.1038/35054508](https://doi.org/10.1038/35054508)
- Tsiganis, K., Gomes, R., Morbidelli, A., & Levison, H. F. 2005, *Natur*, 435, 459. [doi:10.1038/nature03539](https://doi.org/10.1038/nature03539)
- Walsh, K. J., Morbidelli, A., Raymond, S. N., O'Brien, D. P., & Mandell, A. M. 2011, *Natur*, 475, 206. [doi:10.1038/nature10201](https://doi.org/10.1038/nature10201)
- Weissman, P. R. 1983, *A&A*, 118, 90.
- Weissman, P. R. 1996, in *Completing the Inventory of the Solar System*, ed. T. Rettig & J. Hahn, ASP Conf. Ser. Vol. 107, 265.
- Zhang, K., Blake, G. A., & Bergin, E. A. 2015, *ApJL*, 806, L7. [doi:10.1088/2041-8205/806/1/L7](https://doi.org/10.1088/2041-8205/806/1/L7)